

**SLIDING MODE CONTROL OF A SLEWING FLEXIBLE BEAM**David G. Wilson<sup>\*</sup> Gordon G. Parker<sup>†</sup> Gregory P. Starr<sup>‡</sup> Rush D. Robinett III<sup>§</sup>**Abstract**

An output feedback sliding mode controller (SMC) is proposed to minimize the effects of vibrations of slewing flexible manipulators. A spline trajectory is used to generate ideal position and velocity commands. Constrained nonlinear optimization techniques are used to both calibrate nonlinear models and determine optimized gains to produce a rest-to-rest, residual vibration-free maneuver. Vibration-free maneuvers are important for current and future NASA space missions. This study required the development of the nonlinear dynamic system equations of motion; robust control law design; numerical implementation; system identification; and verification using the Sandia National Laboratories flexible robot testbed. Results are shown for a slewing flexible beam.

**Introduction**

For NASA space applications, lightweight robotic manipulators are necessary to reduce launch costs, power consumption, and storage volume of the robot. Slewing structures with long flexible members, such as the Shuttle Remote Manipulator System (RMS) and the Space Station RMS, can excite vibrations. These vibrations can severely degrade the pointing accuracy, thus limiting the speed of rotation and productive use of current and future robotic systems. To achieve good control performance and position precision with current technology requires massive stiff manipulators. Since mass is the strongest driver of launch costs, massive teleoperated systems are unacceptable. Inherent flexibility for manipulator systems is a consequence of launch mass minimization. Flexibility is difficult to model but without its inclusion in the dynamic model, slewing performance will remain poor and control marginally stable. The focus of this research is the development of a robust control system that demonstrates residual-vibration suppression and robust tracking using only collocated joint sensors and actuators. The methodology includes development of the dynamic system equations of motion; sliding mode control system design; optimized model matching and gain calculation; and experimental verification using the Sandia National Laboratories flexible robot testbed.

To find a practical feedback control for flexible arms, many researchers have investigated various control methods. A review of some of these techniques is given in Yeung and Chen.<sup>1</sup> Yeung and Chen also demonstrated successful feedback control of flexible arms using the sliding-mode technique. Nathan and Singh<sup>2</sup> developed a design approach for the control of a flexible robotic arm using variable structure system theory and pole assignment technique for stabilization. The closed-loop system was robust to variations in payload. Qian and Ma<sup>3</sup> have introduced variable structure sliding-mode technique for tip position control. The controller performance was evaluated through simulations. Choi and Shin<sup>4</sup> developed a sliding mode controller for tip position control of a single-flexible link manipulator subjected to parameter variation. Their algorithm showed fast and favorable system responses while maintaining low sensitivity to imposed uncertainties. Parker and Robinett<sup>5</sup> developed an output feedback sliding mode control approach for nonlinear systems in general, with applications to flexible manipulators. Asymptotically stable sliding surfaces are specified in the output space. In addition, a constraint was derived, based on Lyapunov's direct method, ensuring stability of the closed-loop system. The results presented in this paper is a realization of the output feedback sliding mode controller.

---

<sup>\*</sup>Graduate Student, Department of Mechanical Engineering, The University of New Mexico, Albuquerque, NM 87131.

<sup>†</sup>Professor, Michigan Technological University, Houghton, MI 49931.

<sup>‡</sup>Professor, Department of Mechanical Engineering, The University of New Mexico, Albuquerque, NM 87131.

<sup>§</sup>Department Manager, Intelligent Systems Sensors and Control Dept., Sandia National Laboratories, Albuquerque, NM 87185.

## Dynamic Model

The dynamic equations of motion for both the rigid body,  $\theta$  and the flexible body,  $q^i(t)$  degrees-of-freedom (DOF) are found using Lagrange's equations;

$$\frac{d}{dt} \left( \frac{\partial L}{\partial \dot{\theta}} \right) - \frac{\partial L}{\partial \theta} = 0 \quad (1)$$

$$\frac{d}{dt} \left( \frac{\partial L}{\partial \dot{q}^i} \right) - \frac{\partial L}{\partial q^i} = 0 \quad (2)$$

The Lagrangian is,  $L = T - V + W_F$ , where the kinetic energy,  $T$ , the potential energy,  $V$ , and the work from external forces,  $W_F$  are defined as

$$T = \frac{1}{2} \bar{\rho} \int_0^L \dot{\vec{x}}^T \cdot \dot{\vec{x}} dx \quad (3)$$

$$V = \frac{1}{2} (EI) q^i q^j \int_0^L \phi^{i'''}(x) \phi^{j'''}(x) dx \quad (4)$$

$$W_F = \tau q^i \int_0^L \phi^i(x) \eta dx + \tau \theta \quad (5)$$

where  $i$  and  $j = 1$  are the number of flexible DOF and  $x$  is the location along the beam. Applying Lagrange's equations results in the following nonlinear equations of motion;

$$\mathbf{M}(\mathbf{x}) \ddot{\mathbf{x}} + \mathbf{N}(\mathbf{x}, \dot{\mathbf{x}}) + \mathbf{K}(\mathbf{x}, \dot{\mathbf{x}}) = \mathbf{B}(\mathbf{x}) \mathbf{U} \quad (6)$$

$$\mathbf{y} = \mathbf{C} \mathbf{x} \quad (7)$$

where,  $\mathbf{x}$  is an  $n \times 1$  vector of total DOF's,  $\mathbf{M}$  is a  $n \times n$  configuration dependant mass matrix;  $\mathbf{N}$  is a  $n \times 1$  vector of Coriolis and centripetal acceleration terms;  $\mathbf{K}$  is a  $n \times n$  configuration dependant stiffness matrix including centrifugal stiffening terms;  $\mathbf{B}$  is a  $n \times m$  matrix of control weighting coefficients;  $\mathbf{U}$  is a  $m \times 1$  vector of torque inputs;  $\mathbf{y}$  is an  $r \times 1$  vector of measurable outputs,  $\mathbf{C}$  is an  $r \times n$  matrix relating state variables to measurable outputs.

The dynamic equations of motion were developed using the method of quadratic modes.<sup>6</sup> Figure 1 shows a schematic of the slewing flexible beam defining the mathematical geometry.

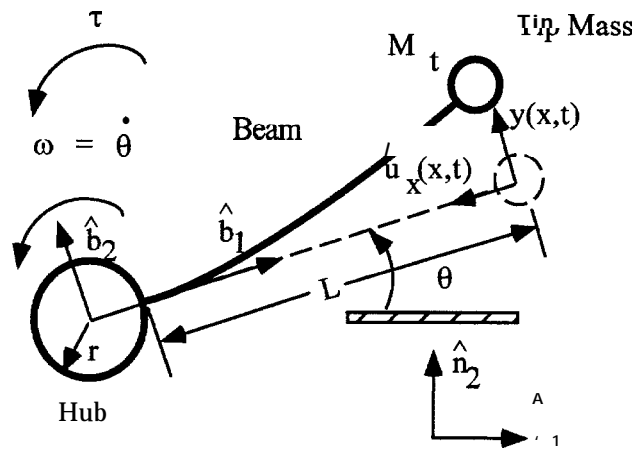


Figure 1: Slewing Flexible Beam Schematic

An expression for the deformation of a point along the beam is

$$\vec{u}(x, t) = u_x(x, t) \hat{b}_1 + y(x, t) \hat{b}_2 \quad (8)$$

where  $\hat{b}_i$  are unit vectors associated with a moving coordinate system attached to the hub. The  $\hat{n}_i$  unit vectors are associated with an inertial coordinate system. Define the following relationships for axial and transverse deflections as

$$u_x(x, t) = -\frac{1}{2} \int_0^x \left( \frac{d y(\xi, t)}{d \xi} \right)^2 d \xi \quad (9)$$

and

$$y(x, t) = \sum_{i=1}^{\infty} \phi^i(x) q^i(t). \quad (10)$$

Equation (10) is assumed to be separable into  $\phi^i(x)$ , the mode shape basis functions and  $q^i(t)$ , the corresponding time-dependent generalized coordinates. The following equation gives the velocity of each point along the rotating beam's length:

$$\dot{\vec{x}}(x, t) = \frac{N_d}{dt} \left\{ [r + x] \hat{b}_1 + \vec{u}(x, t) \right\}. \quad (11)$$

Performing the mathematical expansions and substituting the expressions for the kinetic energy, strain energy, and external work into Lagrange's equations (1,2), we arrive at the following equations for beam deflection and rotation, respectively.

$$\left\{ EI \int_0^L \phi^{i'''}(x) \phi^{j'''}(x) dx - \left( \bar{\rho} \int_0^L \phi^i(x) \phi^j(x) dx + 2\bar{\rho} \int_0^L [r + x] g^{ij}(x) dx \right) \dot{\theta}^2 \right. \\ \left. + \left[ \bar{\rho} \int_0^L \phi^i(x) \phi^j(x) dx \right] \ddot{q}^i + \left[ \bar{\rho} \int_0^L [r + x] \phi^i(x) dx \right] \ddot{\theta} = \tau \int_0^L \phi^i(x) \eta dx \right\} \quad (12)$$

$$\left[ \frac{1}{3} \rho L^3 + \rho r L^2 + \rho r^2 L + M_t(r + L) \right] \ddot{\theta} + \left[ \bar{\rho} \int_0^L (r + x) \phi^i(x) dx \right] \ddot{q}^i = \tau \quad (13)$$

where  $\bar{\rho} = \rho + M_t \delta(x - L)$  and  $\rho$  is mass per unit length.

Cantilever mode shapes given by Blevins<sup>7</sup>, were used for this analysis and the quadratic modes for a beam were defined as;

$$g^{ij} = -\frac{1}{2} \int_0^x \phi^{i'}(\xi) \phi^{j'}(\xi) d\xi. \quad (14)$$

The final equations were arranged into the form of equations (6) and (7).

## Sliding Mode Control

Sliding mode control provides an alternative to robot control with unknown parameters. The main advantage of SMC is its robustness to input disturbances once the sliding surface is reached. SMC uses a strategy whereby the active control law at any given time is chosen from a predefined set of control laws based on the current state of the system. SMC takes advantage of control law switching to move a system from an initial state to a prescribed surface in the state space. Once on that surface, a second control law is used to keep the state from leaving the surface while moving toward the desired final state. Using Lyapunov's direct method, SMC has been shown to be stable<sup>5</sup>. Furthermore, it is robust to model-parameter uncertainty and disturbances if bounds are known a priori. Sliding surfaces are identified for each sensor leading to the output feedback control law. A thorough development of SMC including several practical examples can be found in Utkin.<sup>8</sup>

The sliding surface may be chosen as

$$s = \mathbf{W}(\mathbf{y} - \mathbf{y}_r) + (\dot{\mathbf{y}} - \dot{\mathbf{y}}_r) = 0 \quad (15)$$

where  $\mathbf{y}_r$  is the desired sensor output time history and  $\mathbf{W}$  is a positive definite matrix with real valued elements. The equivalent control is found by enforcing a condition of stationarity on the sliding surface,

$$\dot{s} = \mathbf{W}(\dot{\mathbf{y}} - \dot{\mathbf{y}}_r) + (\ddot{\mathbf{y}} - \ddot{\mathbf{y}}_r) = 0. \quad (16)$$

substituting for  $\mathbf{y}$  from the equations of motion equations (6) and (7), into and solving for  $\mathbf{CM}(\mathbf{x})^{-1}\mathbf{B}(\mathbf{x})\mathbf{U}$  yields;

$$\mathbf{CM}(\mathbf{x})^{-1}\mathbf{B}(\mathbf{x})\mathbf{U} = \mathbf{CM}(\mathbf{x})^{-1}\mathbf{N}(\mathbf{x}, \dot{\mathbf{x}}) + \mathbf{CM}(\mathbf{x})^{-1}\mathbf{K}(\mathbf{x}, \dot{\mathbf{x}}) + \ddot{\mathbf{y}}_r - \mathbf{W}(\dot{\mathbf{y}} - \dot{\mathbf{y}}_r) \quad (17)$$

All terms involving  $\mathbf{x}$  will be approximated with  $\hat{\mathbf{x}}$ , such that

$$\hat{\mathbf{x}} = \mathbf{C}^*\mathbf{y} \quad (18)$$

where  $\mathbf{C}^*$  takes on a form of a psuedo-inverse. In addition to substituting for the estimate of  $\mathbf{x}$  the term  $\mathbf{A}tanh^{-1}(\beta s)$  is added to drive the output to the stable sliding surface of  $s$  and the hyperbolic arctan is used to eliminate chatter through a boundary layer whose slope can be adjusted with  $\beta$ . This results in the final output feedback sliding mode controller;

$$\mathbf{u} = [\mathbf{CM}(\hat{\mathbf{x}})^{-1}\mathbf{B}(\hat{\mathbf{x}})]^{-1}[\mathbf{CM}(\hat{\mathbf{x}})^{-1}\mathbf{N}(\hat{\mathbf{x}}, \dot{\hat{\mathbf{x}}}) + \mathbf{CM}(\hat{\mathbf{x}})^{-1}\mathbf{K}(\hat{\mathbf{x}}, \dot{\hat{\mathbf{x}}}) + \ddot{\mathbf{y}}_r - \mathbf{W}(\dot{\mathbf{y}} - \dot{\mathbf{y}}_r) - \mathbf{A}tanh^{-1}(\beta s)]. \quad (19)$$

Inversion is ensured by setting  $m = r$ . Stability has been established by using Lyapunov's direct method.<sup>5</sup> During the actual implementation of the SMC algorithm the following term was set to zero;

$$\mathbf{CM}(\hat{\mathbf{x}})^{-1}\mathbf{N}(\hat{\mathbf{x}}, \dot{\hat{\mathbf{x}}}) + \mathbf{CM}(\hat{\mathbf{x}})^{-1}\mathbf{K}(\hat{\mathbf{x}}, \dot{\hat{\mathbf{x}}}) = 0. \quad (20)$$

## Optimization

A constrained optimization problem was formulated for the slewing flexible beam involving the physical parameters of the previously derived model and an experimental response to the trajectory input. Solving the trajectory optimization problem involved the use of a recursive quadratic programming algorithm implemented in the MATLAB optimization toolbox.<sup>9</sup> A cost function of the form

$$J = W_1 \int_{t_0}^{t_f} \mathbf{e}_1^T \cdot \mathbf{e}_1 dt + W_2 \int_{t_0}^{t_f} \mathbf{e}_2^T \cdot \mathbf{e}_2 dt \quad (21)$$

subject to a number of inequality constraints  $\mathbf{G}(\mathbf{x}) \leq 0$  was used for both the model matching and the optimized gain analysis.

The model matching optimization errors were set up as  $\mathbf{e}_1 = (\theta_{model} - \theta_{exp})$  and  $\mathbf{e}_2 = (\epsilon_{root_{model}} - \epsilon_{root_{exp}})$ , where  $\epsilon_{root}$  is the strain at the root of the beam. The first step involved setting the parameters belonging to the mass and stiffness properties of the hub and flexible link, The weights were set to  $W_1 = 1.0$  and  $W_2 = 0.0$ . The optimizer was allowed to formulate error predominantly during the rise time  $t_0 = 0.0$  to  $t_f = 0.35$  seconds. After sufficient iterations the parameters would converge to nominal values. The second step was then to concentrate on the friction coefficients as parameters. The optimizer was set-up to work over the settling time portion of the trajectory from  $t_0 = 0.35$  to  $t_f = 0.6$  seconds until the parameters would converge to a nominal value. The third step used a representative set of parameters from both steps one and two. This set of parameters was allowed to only vary between  $\pm 20$  percent. The optimizer worked over the combined time range of the trajectory from  $t_0 = 0.0$  to  $t_f = 0.6$  seconds. Upon successful convergence of these parameters, the rigid body portion of the single flexible link system is identified. The final step included setting  $W_2 \geq 1.0$  and investigating parameters directly associated with the strain location and beam coefficients. This resulted in closer agreement to the experimental setup but was considered only a second-order effect.

For the controller optimization the errors are specified as  $\mathbf{e}_1 = (\theta_c - 6)$  and  $\mathbf{e}_2 = (0.0 - \epsilon_{root})$  where both variables  $\theta_c$  and  $\epsilon_{root}$  are from the simulation model. The optimizer was set up for the hub angle from  $t_0 = 0.0$  to  $t_f = 0.6$  seconds and for the root strain from  $t_0 = 0.4$  to  $t_f = 0.6$  seconds. The cost associated with the root strain is for after the maneuver is completed to minimize residual vibration. For all runs  $W_1 = 1.0$  and  $W_2 = 10$ . To start out, large steps were taken to identify possible minimums. Starting with these minimums the step size was reduced until convergence. These gains were then implemented on the hardware to obtain experimental responses,

## Experimental and Numerical Results

The Sandia National Laboratories flexible robot testbed consists of modular flexible link/motor/hub mounting assemblies; electric DC motors and amplifiers; incremental encoders; bending strain gauges; and a dSPACE<sup>10</sup> real-time control computer and data acquisition system. The slewing flexible beam parameters are given in Table 1.

Parameter	Symbol	Value	Unit
Length	L	48.42	cm
Width	w	7.62	cm
Thickness	t	0.1574	cm.
Hub Radius	r	8.89	cm
Mass Density	$\rho_m$	2700	kg/m <sup>3</sup>
Tip Mass	$M_t$	0.0	kg
Beam Stiff	EI	0.176	kg . m <sup>2</sup>
Motor Inertia	$J_m$	6.92 <sup>-3</sup>	kg . m <sup>2</sup>
Viscous Damp	$b_{vf}$	1.37 <sup>-4</sup>	kg . m <sup>2</sup> /s

Table 1: Slewing Flexible Beam Physical Parameters

A numerical simulation was developed that realized the mathematical models developed earlier. MATLAB was used to implement the differential equations. The dynamics of the plant were treated as continuous states, while the control laws were treated as discrete states. All sampling was performed at 1000 Hz.

The reference motion trajectory of the hub is generated from a spline fit of the initial hub angle, equal to  $-90^\circ$  to the final hub angle, equal to  $90^\circ$ , for the single flexible link case. The time for all the trajectory runs was specified as  $AT = 0.35$  seconds.

### Model Calibration/Matching

The goal of this section was to identify a model that best captured the dynamics of the actual system. A simple PD controller was used to slew the beam. By following the steps outlined in an earlier section, the following plots show the match between the model and the experimental set-up. Using empirically determined gains Figures 2 and 3 show the calibration plots for hub angle, hub velocity, root strain and mid-span strain, respectively.

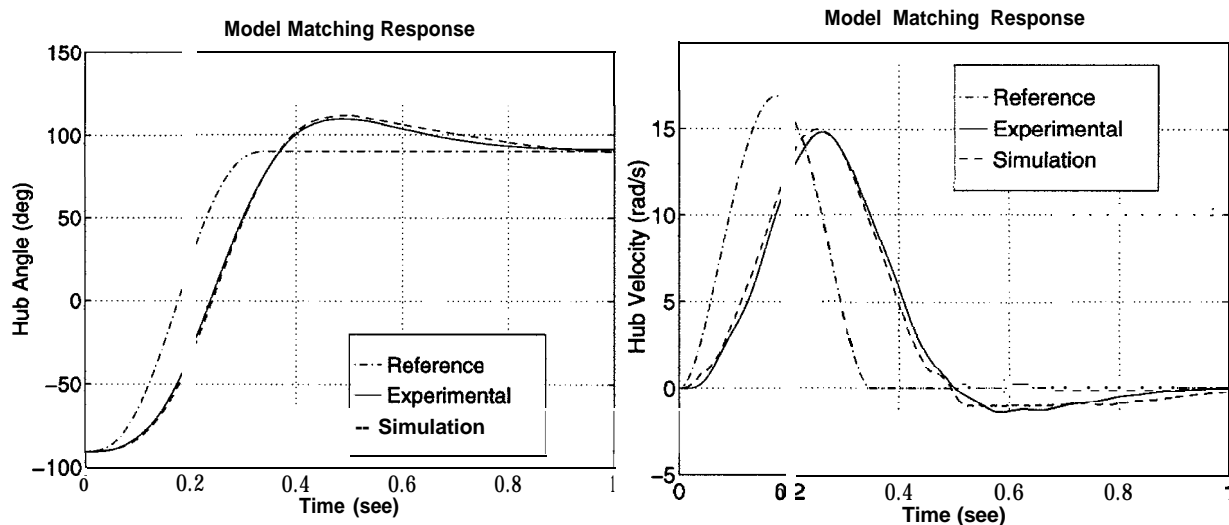


Figure 2: Hub Angle and Velocity Calibration Results

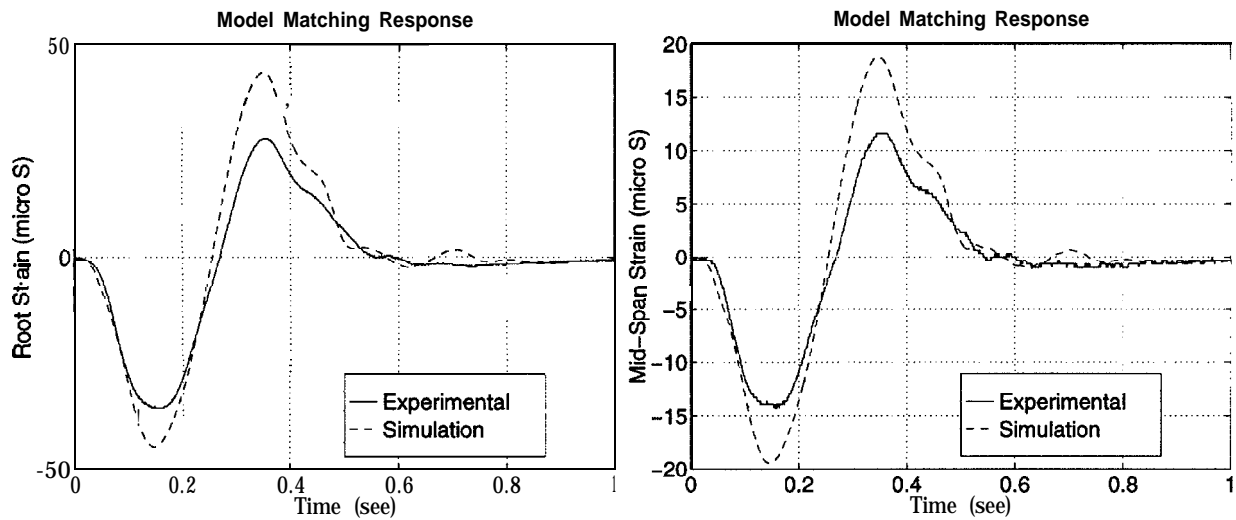


Figure 3: Root and Mid-Span Strain Calibration Results

### Optimized Gains for Controllers

The calibrated model was used to predict the performance of the experimental set-up by using the gains determined from the constrained nonlinear optimization design. The results for the sliding mode control, where the W and A gains were optimized are shown in Figures 4 and 5, for the hub angle, hub velocity, root strain and mid-span strain, respectively.

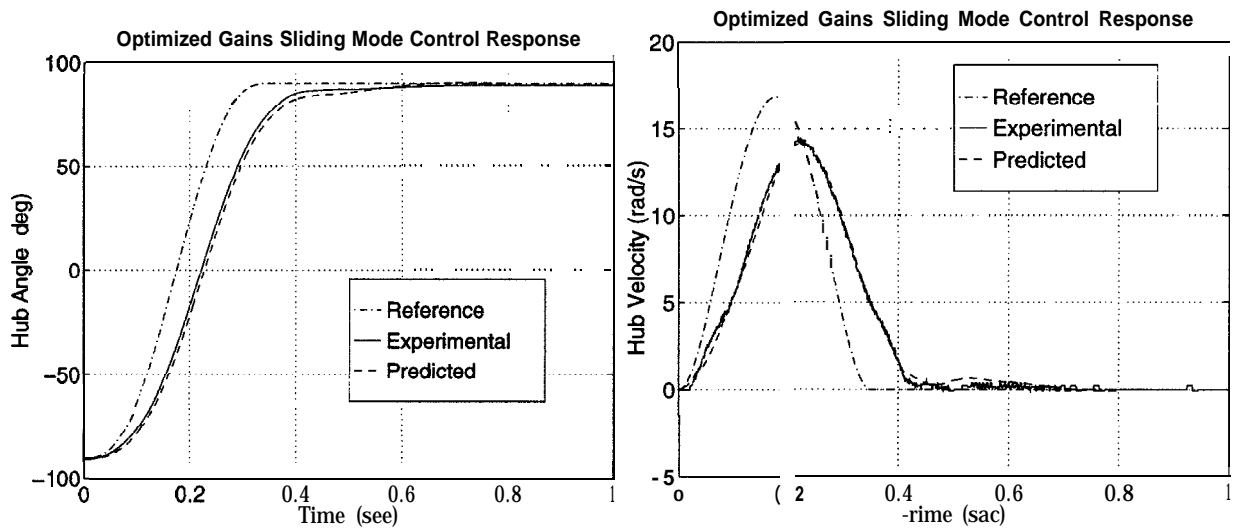


Figure 4: Hub Angle and Velocity Optimized SMC Results

## Conclusions

A sliding mode controller was successfully demonstrated to minimize the effects of vibrations of slewing flexible beams. Optimization techniques were successfully employed to determine meaningful nonlinear time domain models and optimized gain determination. In turn the optimized gains were used to predict flexible beam performance during large angle slews. These optimized gains were experimentally verified on the Sandia National Laboratories flexible robot testbed. The SMC architecture showed minimum residual-vibration suppression and robust tracking using only colocated joint sensors and actuators. Future work will involve the use of 1) piezoceramic strain sensors and actuators<sup>11,12</sup> to enhance stability and tracking performance, and 2) the use of a two DOF planar flexible manipulator.

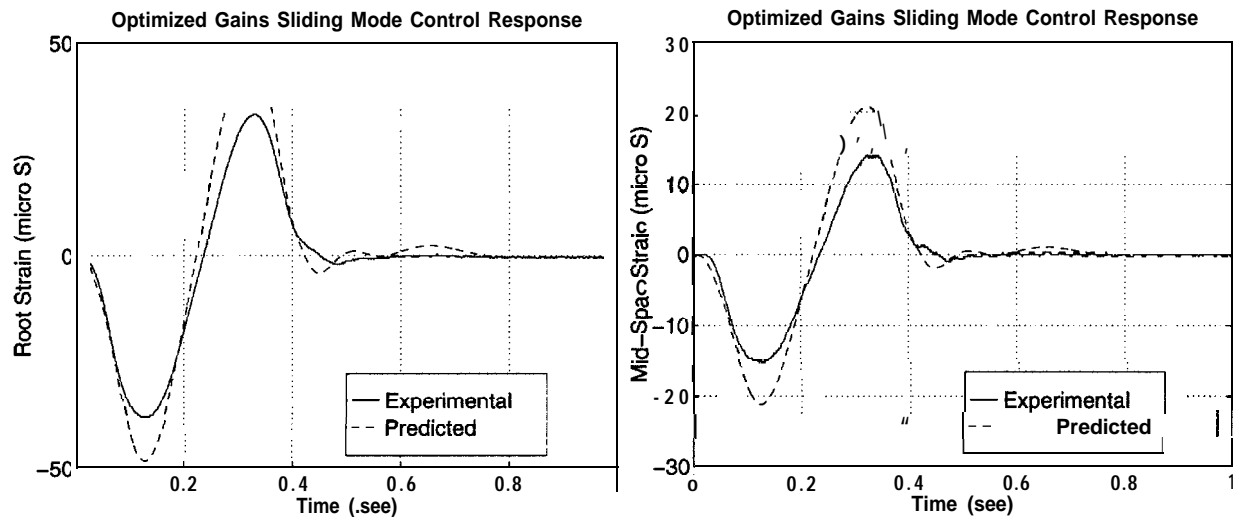


Figure 5: Root and Mid-Span Strain Optimized SMC Results

## Acknowledgements

This work was supported by the U.S. Department of Energy under Contract DE-AC0494AL85000. The first author was also supported through a NASA ACE Fellowship.

## References

- <sup>1</sup>Yeung, K.S. and Chen, Y. P., "Regulation of a One-Link Flexible Robot Arm Using Sliding Mode Technique," *International J. of Control*, **49**, pg. 1965-1978, 1989.
- <sup>2</sup>Nathan, P.J. and Singh, S. N., "Sliding Mode Control and Elastic Mode Stabilization of a Robotic Arm with Flexible Links," *J. of Dynamic Systems, Measurement and Control*, **113**, pg. 667-676, 1991.
- <sup>3</sup>Qian, W.T. and Ma, C. C. H., "A New Controller Design for Flexible One-Link Manipulator," *Transactions on Automatic Control*, **37**, pg. 132-137, 1992.
- <sup>4</sup>Choi, S.-B., Cheong, C.-C., Shin, H.-C., "Sliding Mode Control of Vibration in a Single-Link Flexible Arm with Parameter Variations", *J. of Sound and Vibration*, **179(5)**, pg 737-748, 1995.
- <sup>5</sup>Parker, G. G., Robinett, R. D., "Output Feedback Sliding Mode Control with Application to Flexible Multibody Systems", Submitted to the *Journal of Robotic Systems*, 1996.
- <sup>6</sup>Segalman, D. J., Dohrmann, C. R., "Dynamics of Rotating Flexible Structures by a Method of Quadratic Modes," Sandia National Laboratories, SAND90-2737, December 1990.
- <sup>7</sup>Blevins, R.D., *Formulas for Natural Frequency and Mode Shape*, Krieger Publishing Company, 1993.
- <sup>8</sup>Utkin, V. I., *Sliding Modes in Control Optimization*, Springer-Verlag, 1981.
- <sup>9</sup>Grace, A., *Optimization TOOLBOX for Use with MA TLAB*, The MathWorks, Inc., 1995.
- <sup>10</sup>dSPACE, Real-Time Control System, dSPACE digital signal processing and control engineering GmbH, Technologiepark 25, D-33100 Paderborn, Germany.
- <sup>11</sup>Warren, S. R., Voulgaris, P.G, Bergman, L. A., "Robust Control of a Slewing Beam System", *J. of Vibration and Control*, Vol 1: 251-271, 1995.
- <sup>12</sup>Wilson, D. G., Searle, I., Ikegami, I., and Starr, G. P., "Dynamic Characterization of Smart Structures for Active Vibration Control Applications," *ASME Winter Annual Meeting, Symposium on Vibro-Acoustic Applications*, Nov. 17-22, 1996, Atlanta, Ga.